

# Study on Microhardness, Dynamic Mechanical, and Tribological Properties of PEEK/Al<sub>2</sub>O<sub>3</sub> Composites

R. K. Goyal,<sup>1\*</sup> A. N. Tiwari,<sup>2</sup> U. P. Mulik,<sup>1</sup> Y. S. Negi<sup>3</sup>

<sup>1</sup>Centre for Materials for Electronics Technology, Department of Information Technology, Govt. of India, Panchwati, Off Pashan Road, Pune 411 008, Maharashtra, India

<sup>2</sup>Department of Metallurgy and Materials Science, College of Engineering, Shivaji Nagar, Pune 411 005, India

<sup>3</sup>Polymer Science and Technology Laboratory, Department of Paper Technology, Indian Institute of Technology, Roorkee, Saharanpur Campus, Saharanpur 247 001, Uttar Pradesh, India

Received 14 June 2007; accepted 27 February 2008

DOI 10.1002/app.28925

Published online 11 September 2008 in Wiley InterScience (www.interscience.wiley.com).

**ABSTRACT:** The wear and friction properties of poly(ether-ether-ketone) (PEEK) reinforced with 0–33 vol % (60 wt %) micron size Al<sub>2</sub>O<sub>3</sub> composites were evaluated at a sliding speed of 1.0 m/s and nominal pressure from 0.5 to 1.25 MPa under dry sliding conditions using a pin-on-disk wear tester. The wear resistance of the pure PEEK is 10-fold higher than that of mild steel under the similar test condition. It is improved to 18-fold as compared with mild steel at 3.5 vol % Al<sub>2</sub>O<sub>3</sub> content. The improvement in wear properties may be attributed to the thin, tenacious, and coherent transfer film formed between the steel countersurface and composite pin. However, the wear resistance of PEEK containing above 3.5 vol % Al<sub>2</sub>O<sub>3</sub> was deteriorated, despite their higher hardness and stiffness as compared

with that of composites containing lower Al<sub>2</sub>O<sub>3</sub> content. This is attributed to the formation of thick and noncoherent transfer film, which does not prevent the wear of the composites from hard asperities of countersurface. Moreover, hard Al<sub>2</sub>O<sub>3</sub> particles present in transfer film act as third body wear mechanism. The coefficient of friction of the composites is higher than that of pure PEEK. SEM and optical microscopy have shown that wear of pure PEEK occurs by the mechanism of adhesion mainly whereas of PEEK composites by microploughing and abrasion. © 2008 Wiley Periodicals, Inc. *J Appl Polym Sci* 110: 3379–3387, 2008

**Key words:** composites; microhardness; stiffness; wear; friction; PEEK; Al<sub>2</sub>O<sub>3</sub>

## INTRODUCTION

Poly(ether-ether-ketone), hitherto referred to as PEEK, has been widely used in many applications because of its unique properties such as outstanding thermal, mechanical, chemical, moisture resistant, low coefficient of friction, and high service temperatures properties.<sup>1</sup> It is an attractive material for journal bearings and piston rings under various loading conditions as it is comparatively fatigue resistance and exhibits a low creep rate up to about 250°C.<sup>2,3</sup> Despite its low coefficient of friction, its wear rate often limits its utilization in tribological systems. The wear rate of PEEK was reported to be about 10<sup>-5</sup> mm<sup>3</sup>/N m, which appear to be too large to be used as a mating countersurface material in machinery.<sup>4</sup> However, its wear resistance (inverse of wear rate) can be significantly enhanced by up to two

orders of magnitude by introducing fillers such as carbon fiber,<sup>2</sup> carbon nano fibers,<sup>3</sup> short carbon fibers,<sup>5</sup> CuS,<sup>6</sup> Si<sub>3</sub>N<sub>4</sub>,<sup>7</sup> SiO<sub>2</sub>,<sup>8</sup> SiC,<sup>9–11</sup> ZrO<sub>2</sub>,<sup>12</sup> and Al<sub>2</sub>O<sub>3</sub>.<sup>13</sup> The improved wear resistance was attributed to the smoothing of the countersurface and the developing of a transfer film which results in reduced ability for lowing, tearing, and other nonadhesive components of wear.

The addition of inorganic filler to a polymer has been a common practice to improve the mechanical properties and wear resistance.<sup>14</sup> However, the hardness and strength are not only the factors controlling the wear behavior, but also the nature and stability of the transfer film developed between the sample and countersurface, and its adhesion to the countersurface affects the wear properties.<sup>15,16</sup> The transfer film mainly consists of worn fillers and matrix fragments, which could reduce the direct contact between the sample and countersurface leading to decrease in the contact pressure and the subsurface stress. Under such circumstance the wear resistance is increased provided the transfer film is thin, uniform, and tenacious.<sup>6,8</sup> Wear resistance of polytetrafluoroethylene (PTFE) composites has been improved by more than two orders of magnitude by reinforcing alumina<sup>17</sup> and ZnO nano fillers.<sup>18</sup> However, addition

\*Present address: Department of Metallurgical Engineering, Government College of Engineering, Shivaji Nagar, Pune 411 005, India.

Correspondence to: R. K. Goyal (rkgoyal72@yahoo.co.in) or A. N. Tiwari (ant.iitb@gmail.com).

of ZnO and SiC particles to polyphenylene sulfide deteriorated its wear resistance due to the poor adhesion of the transfer film with the countersurface.<sup>16</sup> This may be due to the fact that the wear resistance significantly depends on many factors such as dispersion state, size, volume fraction, and type of filler particles, surface roughness of the countersurface, and crystallinity of the polymer.<sup>19–21</sup>

Recently, we have demonstrated that the addition of Al<sub>2</sub>O<sub>3</sub> to PEEK matrix increases significantly the thermal stability and modulus.<sup>22,23</sup> It is well-known that Al<sub>2</sub>O<sub>3</sub> is widely used for electronic substrates, heat sinks, and electronic packaging due to its low coefficient of thermal expansion ( $6.6 \times 10^{-6}/^{\circ}\text{C}$ ), high electrical resistivity, high thermal conductivity (30 W/m K), and low dielectric constant.<sup>24</sup> Moreover, it is used to improve wear properties of various polymers. It was, therefore, thought to be worthwhile to explore the effect of the Al<sub>2</sub>O<sub>3</sub> on the wear and friction properties of PEEK. Recently, the effect of nano size Al<sub>2</sub>O<sub>3</sub> on the wear properties of PEEK matrix was studied.<sup>13,25</sup> Nevertheless, wear behavior of composite depends upon size and loading of reinforcing particles and its adhesion with the matrix. For this purpose, PEEK matrix composites reinforced with micron size (7.8  $\mu\text{m}$ ) Al<sub>2</sub>O<sub>3</sub> particles ranging from 0 to 33 vol % (60 wt %) were prepared by hot pressing and their wear and friction properties were evaluated using pin-on-disk wear tester. In addition to this, microhardness and dynamic mechanical properties were also evaluated.

## EXPERIMENTAL

### Materials

A commercial PEEK (grade 5300PF) donated by Gharda Chemicals Ltd. Panoli, Gujarat, India under the trade name GATONE™ PEEK was used as matrix in the present study. The Aluminum oxide (Al<sub>2</sub>O<sub>3</sub>) purchased from Aldrich Chemical Company was used as reinforcement without surface treatment. Ethanol from Merck was used for homogenizing the Al<sub>2</sub>O<sub>3</sub> and PEEK mixture. The mean particle size of the PEEK and Al<sub>2</sub>O<sub>3</sub> was 25 and 7.8  $\mu\text{m}$ , respectively.

### Preparation

Various compositions of PEEK reinforced with 0–33 vol % Al<sub>2</sub>O<sub>3</sub> were prepared using the method described in our previous article.<sup>22</sup> Dried powder of Al<sub>2</sub>O<sub>3</sub> and PEEK were well premixed through magnetic stirring using an ethanol medium and the resultant powder was dried in an oven at 120°C to remove the ethanol. The pure PEEK and its composite samples were prepared by using a laboratory hot

press under a pressure of 15 MPa and 350°C. Composite samples were coded by AOM-X, where AOM and X are Al<sub>2</sub>O<sub>3</sub> and wt % of Al<sub>2</sub>O<sub>3</sub> in PEEK matrix, respectively.

### Characterization

Theoretical density of the samples was calculated by rule of mixture using the density of Al<sub>2</sub>O<sub>3</sub> 4.00 g/cm<sup>3</sup> and of PEEK 1.29 g/cm<sup>3</sup> for 20% crystalline powder. Experimental density of the filled PEEK samples was measured by Archimedes method. The relative density is the ratio of the experimental density to the theoretical density.

Microhardness test (Model: DVK-2S, Matsuzawa Seiki Co. Ltd. Tokyo) with a Vickers diamond pyramidal indenter was used to determine the microhardness of composites under a constant load of 100 g and a dwell time of 15 s. The average of the three hardness readings was reported as the microhardness of the samples.

The dynamic mechanical tests were carried out in the three point bending mode using a Perkin–Elmer DMA 7e dynamic mechanical analyzer from 30 to 250°C at a heating rate of 5°C/min and a frequency of 1 Hz. The specimen platform has a span length of 15 mm. The bending aspect ratio, i.e., ratio of span length to sample thickness, of samples was about 15. The test was carried out in argon atmosphere under static load of 110 mN and a dynamic load of 100 mN. Before starting the cycle, the samples were held for 5 min at 30°C to stabilize the position of the knife. The interfacial adhesion between the particles and polymer matrix can be estimated by Kubat parameter (A)<sup>26</sup> using eq. (1).

$$A = \{[\tan \delta_c / (V_m \tan \delta_m)] - 1\} \quad (1)$$

where  $\tan \delta_c$  and  $\tan \delta_m$  are the damping of the composite and matrix, respectively. It is reported that  $A$  approaching to 0 corresponds to strong interfacial bonding between the particles and the matrix in the composites.

Wear rate and coefficient of friction were conducted on a pin-on-disk wear tester at a sliding speed of 1.0 m/s and nominal pressure of 0.5–1.25 MPa. The tests were conducted for a total sliding distance of 9 km, which were divided into three stages with 3 km each cycle. The EN-24 steel (C: 0.4%, Si: 0.2%, Mn: 0.6%, Ni: 1.5%, Cr: 1.2%, Mo: 0.3%, and Fe: bal.) disk of diameter 76.48 and 5 mm thick was used as a countersurface. It was heat treated to harden to  $R_c$  50–52. The disk surface was abraded with water proof SiC paper to a surface roughness of  $R = 0.06 \mu\text{m}$ . The surface of the countersurface and pin was cleaned thoroughly with cotton dipped in acetone. The test was performed

TABLE I  
Density of PEEK/Al<sub>2</sub>O<sub>3</sub> Composites

Sample code	Al <sub>2</sub> O <sub>3</sub> in PEEK		Theoretical density (g/cm <sup>3</sup> )	Experimental density (g/cm <sup>3</sup> )	Relative density (%)
	wt %	vol %			
AOM-0	0	0	1.290	1.304	101.1
AOM-5	5	1.67	1.335	1.358	101.7
AOM-10	10	3.46	1.384	1.384	100.0
AOM-20	20	7.46	1.463	1.507	103.0
AOM-30	30	12.14	1.619	1.621	100.1
AOM-50	50	24.39	1.951	1.946	99.7
AOM-60	60	32.60	2.174	2.117	97.4

under a  $48 \pm 2$  relative humidity and 30°C condition. The composite pin height losses were measured by measuring height to an accuracy of 1  $\mu$ m. The height loss versus nominal pressure was plotted for each composite. To determine the specific wear rate a linear regression line is fitted to data by using the method reported in our previous article.<sup>13</sup> To investigate the role of transfer film on wear rate, the specific wear rate of mild steel was also determined under the similar test conditions.

Scanning electron microscopy (SEM) (Philips XL-30) was used to examine the worn surface of the composite pins and wear debris. SEM was also used to examine the morphology of PEEK powder, Al<sub>2</sub>O<sub>3</sub> powder, and composite samples. The AOM-0, AOM-30, and AOM-50 composite samples were fractured in liquid nitrogen to observe the Al<sub>2</sub>O<sub>3</sub> particles distribution in PEEK matrix. All samples were coated with a thin layer of gold to make them electrically conductive prior to examining on SEM. Energy dispersive spectroscopy (EDS) was used to test the elemental composition of the contact surface of the composite. The transfer films formed between the pin and countersurface were examined by optical microscopy (Nikon).

## RESULTS AND DISCUSSION

### Density

Table I shows theoretical and experimental density of the PEEK/Al<sub>2</sub>O<sub>3</sub> composites. The experimental density of the composites is slightly higher than that of theoretical density below 24.4 vol % Al<sub>2</sub>O<sub>3</sub> reinforced PEEK, which may be attributed to porosity free samples and slightly increased crystallinity of PEEK as a result of nucleating effect of Al<sub>2</sub>O<sub>3</sub>.<sup>22</sup> However, the experimental density of the PEEK containing 24.4 vol % and more Al<sub>2</sub>O<sub>3</sub> is lower than that of theoretical density. This may be due to the presence of porosity in the samples. As more and more Al<sub>2</sub>O<sub>3</sub> is added into PEEK, inter particle-particle distance is decreased, which results in aggregation of particles. These aggregates hinder the infiltration of molten PEEK due to its high melt vis-

cosity, hence results in porosity in the PEEK composites containing higher Al<sub>2</sub>O<sub>3</sub>.

### Microhardness

Figure 1 shows the microhardness of PEEK/Al<sub>2</sub>O<sub>3</sub> composites as a function of Al<sub>2</sub>O<sub>3</sub> content. The hardness of composites increases from 24 kg/mm<sup>2</sup> for the pure PEEK to 35 kg/mm<sup>2</sup> for AOM-60 composite. This indicates that load carrying capacity of the composites is improved with increasing Al<sub>2</sub>O<sub>3</sub> content. The uniform distribution of Al<sub>2</sub>O<sub>3</sub> particles in PEEK matrix, as discussed in SEM section, may result in increase of resistance to indentation of PEEK matrix. Nevertheless, the inter particle-particle distance decreases with increasing Al<sub>2</sub>O<sub>3</sub> content, which can resist well the local plastic deformation of the PEEK matrix. Moreover, increase in PEEK crystallinity<sup>22</sup> and higher microhardness of Al<sub>2</sub>O<sub>3</sub> (2000 kg/mm<sup>2</sup>) as compared to pure PEEK might increase the microhardness of the composites.

### Dynamic mechanical properties

It is well-known that dynamic mechanical properties are highly sensitive to the structure of materials. Therefore, they were studied from room temperature

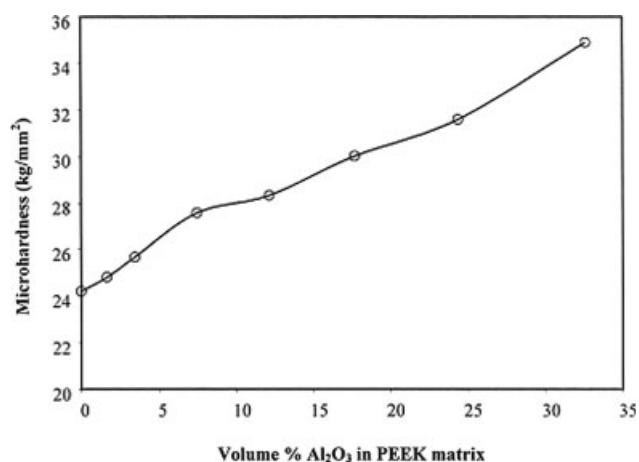
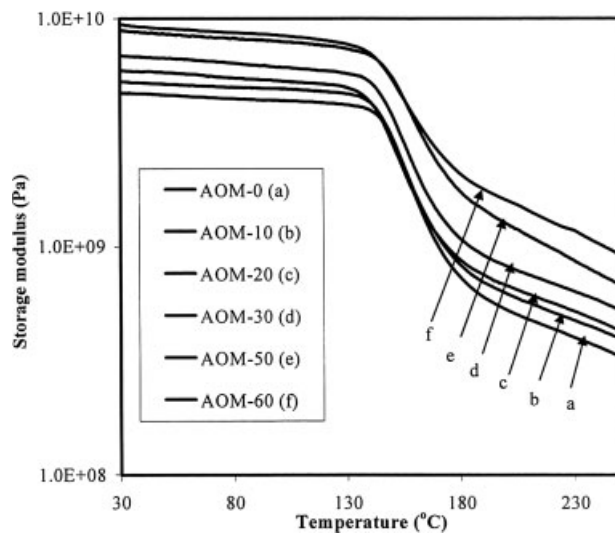


Figure 1 Microhardness as a function of Al<sub>2</sub>O<sub>3</sub> in PEEK matrix.



**Figure 2** Storage modulus as a function of temperature for PEEK/Al<sub>2</sub>O<sub>3</sub> composites.

to 250°C at a heating rate of 5°C/min under argon temperature. Figures 2 and 3 show storage modulus and  $\tan \delta$  as a function of temperature for the PEEK/Al<sub>2</sub>O<sub>3</sub> composites, respectively. As expected, the storage modulus increases with increasing Al<sub>2</sub>O<sub>3</sub> content in PEEK matrix. The modulus is increased due to the high modulus of Al<sub>2</sub>O<sub>3</sub> (345 GPa) and from the interface formed between the Al<sub>2</sub>O<sub>3</sub> and the matrix. The glass transition temperature ( $T_g$ ) of PEEK was characterized by the temperature at the peak of  $\tan \delta$ . The  $T_g$  increases from 155°C for the pure PEEK to 161°C for AOM-50. The  $\tan \delta$  of composites at  $T_g$  is lower than that of the pure PEEK matrix. This may be attributed to the increased crystallinity and reduced fraction of PEEK in the composites. Table II shows that Kubat parameter calculated for the AOM-10 composite is very close to 0, which indicates strong adhesion between the Al<sub>2</sub>O<sub>3</sub> particles and the PEEK matrix. However, for composites containing higher than 3.5 vol % Al<sub>2</sub>O<sub>3</sub>, the Kubat parameter is more than 0, which imply poor adhesion between the Al<sub>2</sub>O<sub>3</sub> particles and the PEEK matrix.<sup>26,27</sup>

### Wear testing

The specific wear rates for the mild steel, PEEK, and PEEK/Al<sub>2</sub>O<sub>3</sub> composites are shown in Figure 4. The specific wear rate of pure PEEK and mild steel is 9.7

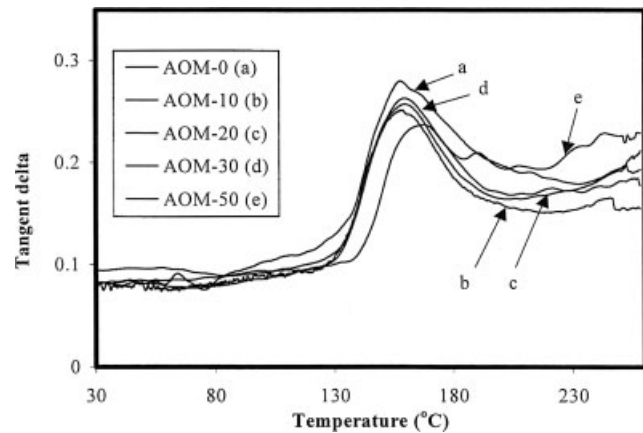


**Figure 3** Tangent  $\delta$  as a function of temperature for PEEK/Al<sub>2</sub>O<sub>3</sub> composites.

$\times 10^{-6}$  mm<sup>3</sup>/N m and  $95 \times 10^{-6}$  mm<sup>3</sup>/N m, respectively, under the similar test condition. In other words, the specific wear rate of mild steel is one order of magnitude higher than that of pure PEEK. This is despite much higher Vickers microhardness of mild steel (125 kg/mm<sup>2</sup>) as compared with that of pure PEEK (24 kg/mm<sup>2</sup>). It may be due to the poor transfer film of mild steel on the countersurface. This indicates that the transfer film formed by sliding PEEK or its composites is very important and effective in improving the wear resistance of the materials. This study shows that transfer film developed during sliding wear has major role compared with sample hardness. Figure 4 shows that the specific wear rate of composites reaches to minimum level, i.e.,  $5.2 \times 10^{-6}$  mm<sup>3</sup>/N m at 3.5 vol % Al<sub>2</sub>O<sub>3</sub> (AOM-10). In other words, the wear rate of AOM-10 composite is decreased by twofold and 18-fold approximately as compared to pure PEEK and mild steel, respectively. When the Al<sub>2</sub>O<sub>3</sub> content is more than 3.5 vol % the wear rate increases drastically and becomes even higher than that of mild steel at  $\sim 33$  vol % Al<sub>2</sub>O<sub>3</sub> content. This is happened despite their higher hardness and stiffness as compared with that of composites containing lower volume fraction of Al<sub>2</sub>O<sub>3</sub>.

### Friction testing

Figure 5 shows the variation of coefficient of friction of the PEEK/Al<sub>2</sub>O<sub>3</sub> composites as a function of load. The coefficient of friction for pure PEEK and its composites decreases with increasing load. For

**TABLE II**  
Kubat Parameter (A) of PEEK/Al<sub>2</sub>O<sub>3</sub> Composite

Compositions	AOM-0	AOM-10	AOM-20	AOM-30	AOM-50	AOM-60
Parameter (A)	0	-0.004	0.08	0.140	0.210	0.320

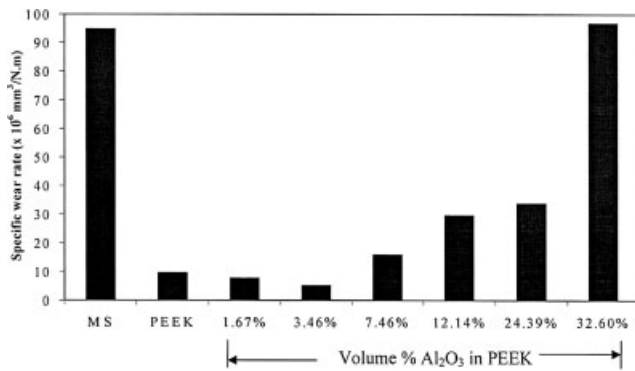


**Figure 4** Specific wear rate for mild steel (MS), PEEK, and PEEK/Al<sub>2</sub>O<sub>3</sub> composites (Sliding speed: 1 m/s, sliding distance: 9 km).

viscoelastic materials, the variation of coefficient of friction with applied load follows eq. (2).

$$M = KN^{(n-1)} \quad (2)$$

where  $K$  and  $n$  ( $2/3 < n < 1$ ) are the constant, and  $N$  is the applied load. According to this equation, the coefficient of friction decreases with increasing load.<sup>15</sup> The coefficient of friction of all composites except AOM-30 is almost higher than that of pure PEEK. This is similar to the results of PEEK/CuO,<sup>6</sup> PTFE/Ni,<sup>15</sup> poly(phthalazine ether sulfone ketone)

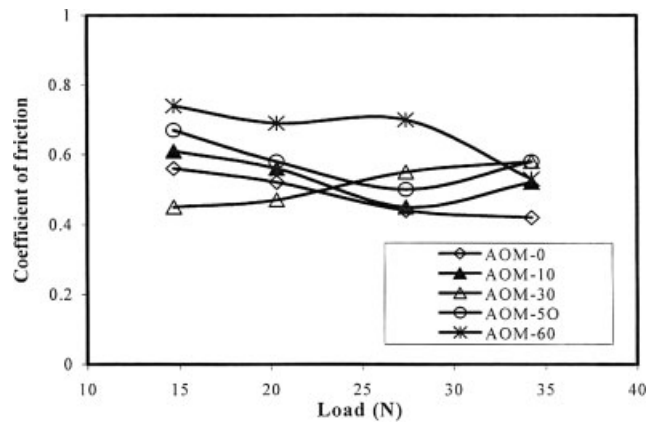


**Figure 5** Coefficient of friction as a function of load for PEEK/Al<sub>2</sub>O<sub>3</sub> composites (Sliding speed: 1 m/s, sliding distance: 9 km).

(PPESK)/micro-TiO<sub>2</sub>,<sup>28</sup> and PPESK/nano-Al<sub>2</sub>O<sub>3</sub><sup>29</sup> composites. The friction coefficient of AOM-30 is lower than that of pure PEEK and other composites below 25 N load whereas it is increased to a value higher than pure PEEK above 25 N. The higher friction of composites may be attributed to the increased contribution to the deformation components of friction by the hard Al<sub>2</sub>O<sub>3</sub> particles during sliding against the composite, i.e., microploughing due to the third body abrasion.<sup>6</sup>

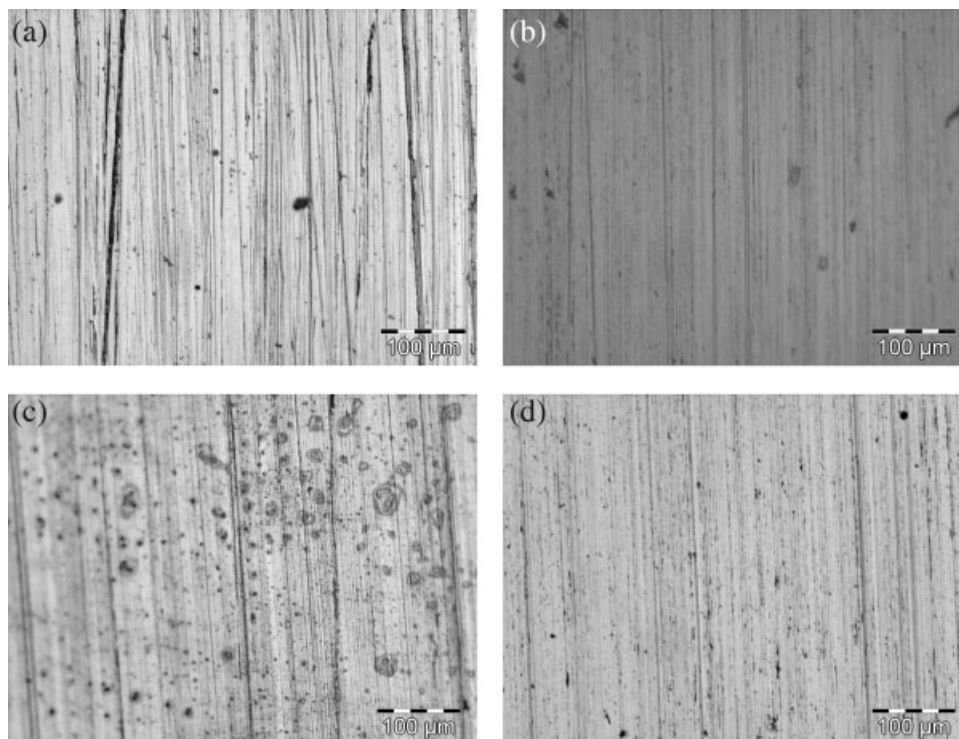


**Figure 6** Optical micrographs of transfer films developed on steel countersurface during sliding wear for (a) as polished countersurface, (b) AOM-0 (PEEK), (c) AOM-10, and (d) AOM-60. Arrow shows sliding direction. (Sliding speed: 1 m/s, sliding distance: 3 km, Load: 25 N).

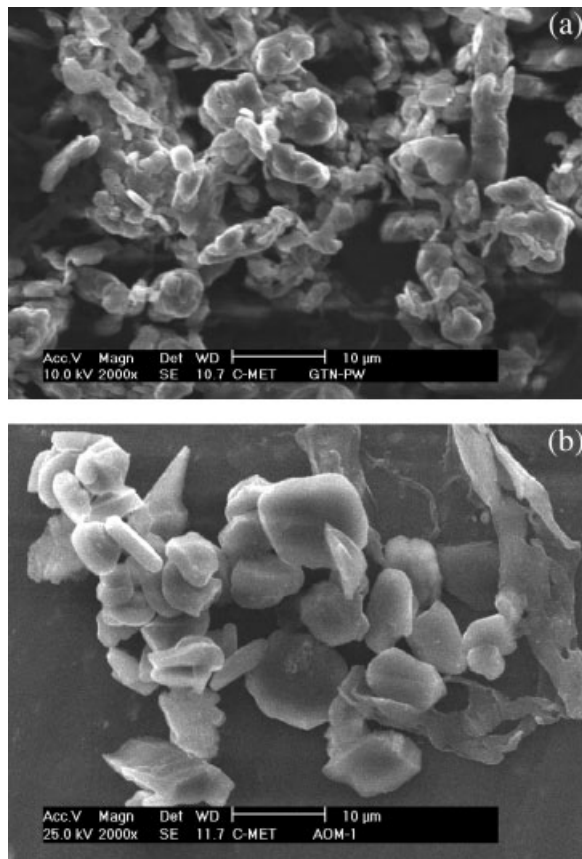


**Figure 7** SEM of (a) PEEK powder and (b)  $\text{Al}_2\text{O}_3$  powder (Scale bar: 10  $\mu\text{m}$ ).

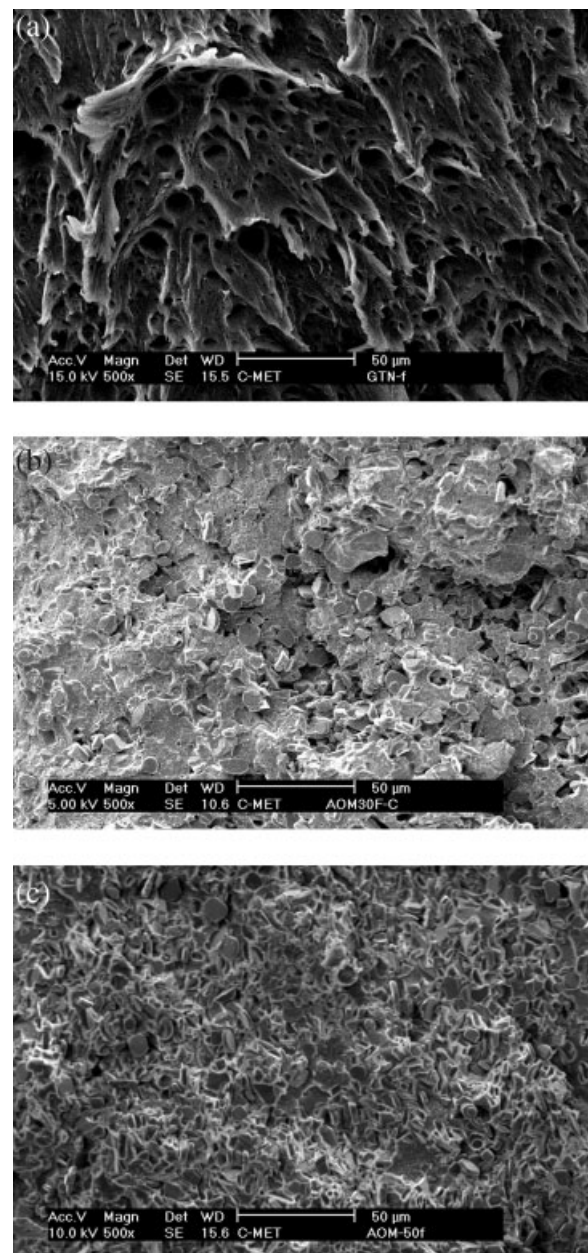
### Study of transfer films

Figure 6 shows the nature of transfer film formed on the countersurface due to sliding wear of composites. Figure 6(a) shows the initial surface of the countersurface in as polished condition. Figure 6(b–d) shows the transfer films developed after 3 km sliding by AOM-0 (PEEK), AOM-10, and AOM-60 composites, respectively. Figure 6(b) shows that pure PEEK forms a continuous transfer film, which covers trough and asperities of the countersurface effectively. In the case of AOM-10 composite, formation of a thin, tenacious, and uniform transfer film occurs as shown in Figure 6(c). This contributes to a marginal decrease in specific wear rate. However, in case of AOM-30 composite thick, lumpy, and non-uniform transfer film was observed visually. Similarly during sliding wear of AOM-60 composite, there was hardly any development of transfer film on the countersurface as shown in Figure 6(d). In addition, some grooves can be seen on countersurface. This might be due to the poor adhesion strength of transfer film with countersurface<sup>17,30,31</sup> and much higher hardness of  $\text{Al}_2\text{O}_3$  than countersurface. It is well-known that at higher ceramic particle loading particle–particle interaction occurs, which

results in aggregation of particles. The resultant ceramic aggregates hinder the formation of a continuous transfer film and results in dramatic increase in wear rate of corresponding composites.

### SEM study on worn composite pins

Figure 7 shows the morphology of pure PEEK and  $\text{Al}_2\text{O}_3$  powder. As shown in Figure 7(a), PEEK has irregular particles of rod-like shape of length ranging from 10 to 50  $\mu\text{m}$ . Figure 7(b) shows flat platelet shaped  $\text{Al}_2\text{O}_3$  particles. Size of the  $\text{Al}_2\text{O}_3$  particles ranged from 3 to 15  $\mu\text{m}$ . Figure 8 shows SEM of AOM-0, AOM-30, and AOM-50 samples fractured in



**Figure 8** SEM of Fractured surfaces of (a) AOM-0, (b) AOM-30, and (c) AOM-50 (Scale bar: 50  $\mu\text{m}$ ).

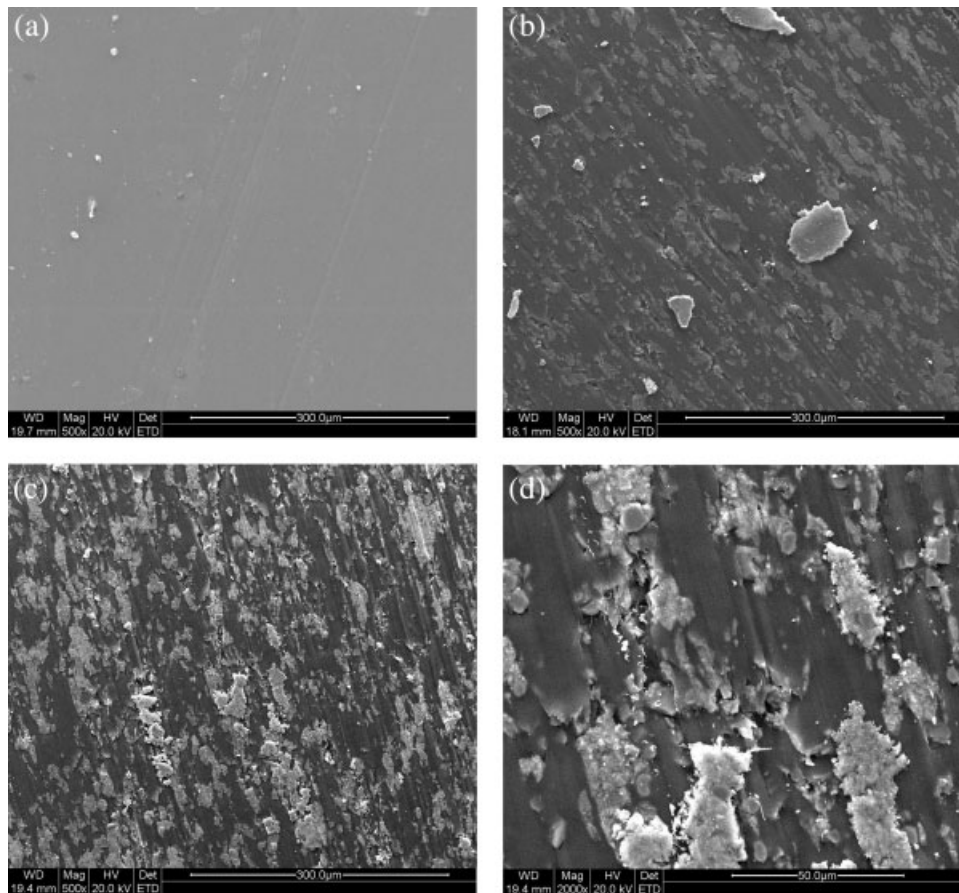


**Figure 9** SEM of worn surfaces of (a) AOM-0, (b) AOM-30, and (c, d) AOM-60; Scale bar: 300  $\mu\text{m}$  (a–c) and 50  $\mu\text{m}$  (d) (Sliding speed: 1 m/s, sliding distance: 3 km, Load: 25 N).

liquid nitrogen. It can be seen that Al<sub>2</sub>O<sub>3</sub> particles are uniformly distributed in PEEK matrix. There are no aggregates of Al<sub>2</sub>O<sub>3</sub> particles in composites containing up to 24.4 vol % Al<sub>2</sub>O<sub>3</sub>, which is expected due to good processing condition during the sample preparation.

The SEM micrographs of the worn surfaces of the pure PEEK and its composites are shown in Figure 9. The worn surface of pure PEEK shows sign of adhesive wear as shown in Figure 9(a), which may be due to the removal of flaky or lamellae-like debris from the pure PEEK surface. This indicates that adhesion is the dominant wear mechanism for pure PEEK. In contrast, Figure 9(b,c) show mild and severe abrasive wear for AOM-30 and AOM-60, respectively. From Figure 9(d), the pull out of Al<sub>2</sub>O<sub>3</sub> particles and some cracks can be seen clearly on the worn surface of AOM-60. This is attributed to the presence of porosity, which is prone to crack initiation and growth during successive sliding wear. Moreover, poor adhesion between the Al<sub>2</sub>O<sub>3</sub> particles and PEEK matrix as confirmed from Kubat parameter might cause pull out of Al<sub>2</sub>O<sub>3</sub> particles from PEEK matrix.

The SEM micrographs of the debris of the mild steel, AOM-0, AOM-10, and AOM-20 samples are shown in Figure 10(a–d), respectively. Figure 10(a) shows that the size of wear debris generated by mild steel is from few microns to more than 50  $\mu\text{m}$ . The wear debris has sharp edges, which results in much higher wear rate as compared with pure PEEK and its composites. The sample AOM-0 that is pure PEEK transfers lumpy flaky or lamellae-like debris on the steel counter-face during wearing because these debris can be easily removed during subsequent wear. The size of AOM-10 and AOM-20 composite debris is smaller than that of pure PEEK. As the Al<sub>2</sub>O<sub>3</sub> content in PEEK increases debris particle size decreases. The size of debris for AOM-50 and AOM-60 was very fine and hence, could not be collected for SEM study.

#### Energy dispersive spectroscopy

Energy dispersive spectroscopy (EDS) was conducted on the worn surface of AOM-30 composite pin. In the EDS spectra (Fig. 11), some

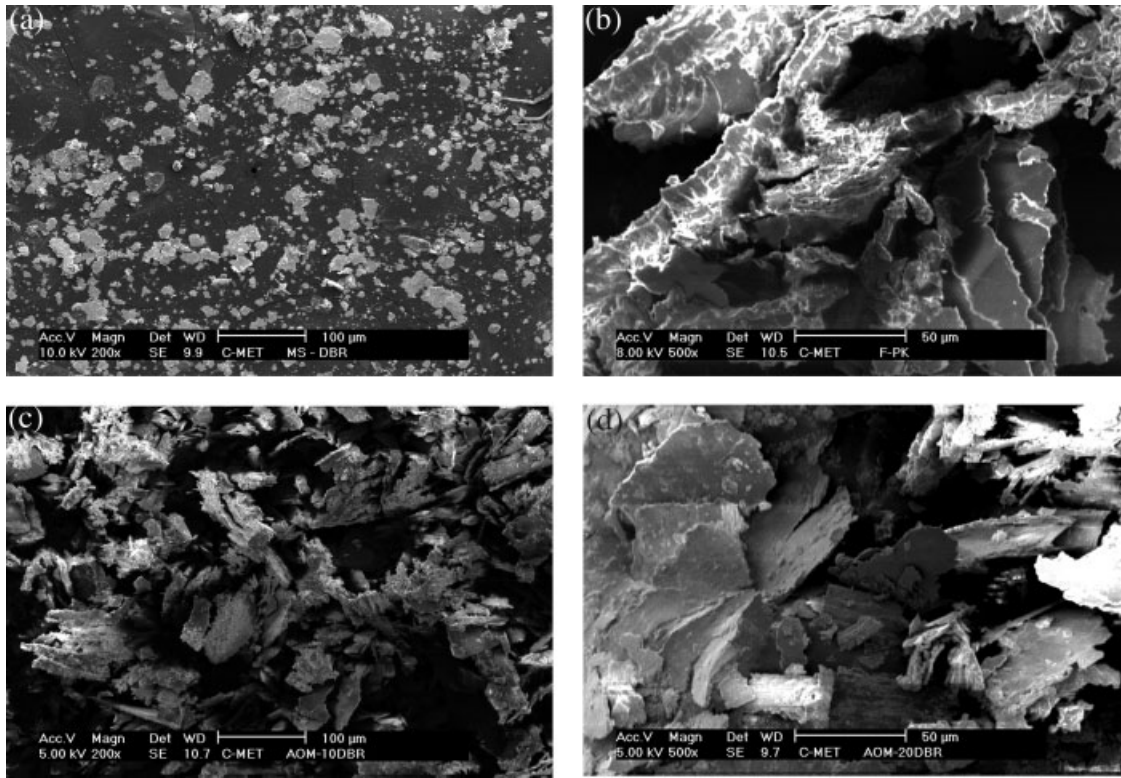


**Figure 10** SEM of wear debris of (a) mild steel, (b) AOM-0, (c) AOM-10, and (d) AOM-20 (Scale bar; 50 μm) (Sliding speed: 1 m/s, sliding distance: 3 km, Load: 25 N).

concentration of Al element exists along with majority of Fe element. This revealed that Al<sub>2</sub>O<sub>3</sub> particle and Fe element were transferred from the composite pin and countersurface, respectively, to the contact surface of composite pin. Moreover, some alloying elements of countersurface such as Si, Mo, Cr, and Mn were also observed. The transfer of Fe and alloying element to contact surface at higher Al<sub>2</sub>O<sub>3</sub> content represents fresh regenerate of track due to abrasive action of Al<sub>2</sub>O<sub>3</sub>, which results in increased wear rate.

## CONCLUSIONS

On the basis of the above investigations, the following conclusions can be drawn.

1. The experimental density of the composites is slightly higher than that of theoretical density below 24.4 vol % Al<sub>2</sub>O<sub>3</sub> content whereas, it is lower than that of theoretical density for composites containing 24.4 vol % and more Al<sub>2</sub>O<sub>3</sub>.
2. The microhardness and stiffness of the composites increases with increasing Al<sub>2</sub>O<sub>3</sub> content

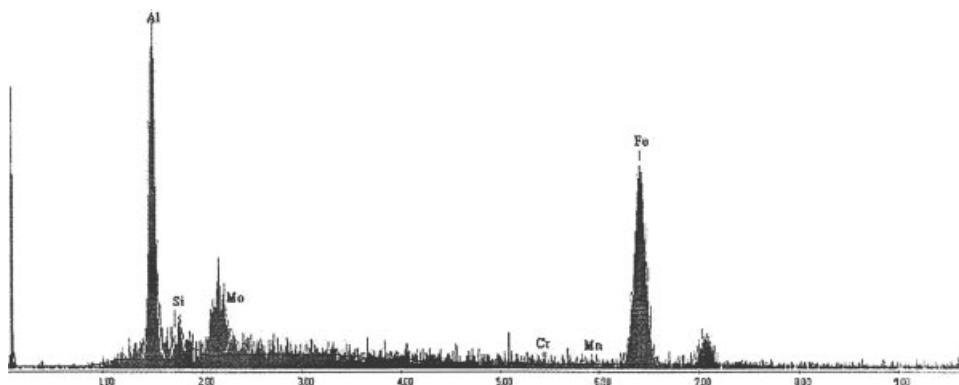


**Figure 11** EDS of worn AOM-30 composite surface.



3. Wear resistance of PEEK sliding against EN-24 steel countersurface is about 10-folds as compared with mild steel under the similar test conditions. It is increased to about 18-folds at 3.5 vol % micron size Al<sub>2</sub>O<sub>3</sub> content. The improvement in wear resistance is attributed to the increased stiffness of composites, and formation of a thin and coherent transfer film.
4. Wear resistant of PEEK composites containing above 3.5 vol % Al<sub>2</sub>O<sub>3</sub> decreases with increasing Al<sub>2</sub>O<sub>3</sub>. It becomes even higher than that of mild steel at ~ 33 vol % Al<sub>2</sub>O<sub>3</sub> content despite its highest hardness and stiffness among composites. This is attributed to the poor quality transfer film and third body wear mechanism.
5. There is no direct correlation between hardness/stiffness and wear rate.
6. Coefficient of friction of composites is higher than that of pure PEEK. It is highest for the PEEK containing 33 vol % Al<sub>2</sub>O<sub>3</sub>. The composite containing 3.5 vol % Al<sub>2</sub>O<sub>3</sub> can be used for a good fractional material.

We thank Dr. P. D. Trivedi, Polymer Division, Gharda Chemicals, India for providing PEEK powder for this research work. We are grateful to Dr. T. L. Prakash, Executive Director of C-MET for his active interest in this work.

## References

1. Frederic, N. C. *Thermoplastic Aromatic Polymer Composites*; Butterworth Heinemann Ltd.: Oxford, 1992.
2. Lu, Z. P.; Friedrich, K. *Wear* 1995, 181–183, 624.
3. Werner, P.; Altstädt, V.; Jaskulka, R.; Jacobs, Q.; Sandler, J. K. B.; Shaffler, M. S. P.; Windle, A. H. *Wear* 2004, 257, 1006.
4. Yamamoto, Y.; Hashimoto, M. *Wear* 2004, 257, 181.
5. Hanchi, J.; Eiss, N. S., Jr. *Wear* 1997, 203/204, 380.
6. Bahadur, S.; Gong, D. *Wear* 1992, 154, 151.
7. Wang, Q. H.; Xu, J.; Shen, W.; Liu, W. *Wear* 1996, 196, 82.
8. Wang, Q.; Xue, Q.; Shen, W. *Tribol Int* 1997, 30, 193.
9. Bahadur, S.; Gong, D.; Anderegg, J. W. *Wear* 1993, 160, 131.
10. Wang, Q. H.; Xu, Q.; Liu, W.; Shen, W. *J Appl Polym Sci* 1999, 74, 2611.
11. Wang, Q. H.; Xu, Q.; Shen, W. *J Appl Polym Sci* 1998, 69, 2341.
12. Wang, Q. H.; Xu, J.; Liu, H.; Shen, W.; Xu, J. *Wear* 1996, 198, 216.
13. Goyal, R. K.; Tiwari, A. N.; Negi, Y. S. *Mater Sci Eng: A* 2008, 486, 602.
14. Zhang, R.; Häger, A. M.; Friedrich, K.; Song, Q.; Dong, Q. *Wear* 1995, 181–183, 613.
15. Zhang, Z.-Z.; Xue, Q. J.; Liu, W.-M.; Shen, W.-C. *Wear* 1997, 210, 151.
16. Bahadur, S.; Sunkara, C. *Wear* 2005, 258, 1411.
17. Sawyer, W. G.; Freudenberg, K. D.; Bhimaraj, P.; Schadler, S. *Wear* 2003, 254, 573.
18. Li, F.; Hu, K.; Li, J.; Zhao, B. *Wear* 2002, 249, 877.
19. Rong, M. Z.; Zhang, M. G.; Liu, H.; Zeng, H. M.; Werzel, B.; Friedrich, K. *Ind Lubr Tribol* 2001, 53, 72.
20. Durand, J. M.; Vardavouliar, M.; Jeandin, M. *Wear* 1995, 181–183, 833.
21. Schwartz, C. J.; Bahadur, S. *Wear* 2000, 237, 261.
22. Goyal, R. K.; Negi, Y. S.; Tiwari, A. N. *J Appl Polym Sci* 2006, 100, 4623.
23. Goyal, R. K.; Tiwari, A. N.; Mulik, U. P.; Negi, Y. S. *J Appl Polym Sci* 2007, 104, 568.
24. Hill, R. F.; Supancic, P. H. *J Am Ceram Soc* 2004, 87, 1831.
25. Qiao, H.-B.; Guo, Q.; Tian, A.-G.; Pan, G.-L.; Xu, L.-B. *Tribol Int* 2007, 40, 105.
26. Kubat, J.; Rigdahl, M.; Welander, M. *J Appl Polym Sci* 1990, 39, 1527.
27. Shi, G.; Zhang, M. Q.; Rong, M. Z.; Wetzell, B.; Friedrich, K. *Wear* 2003, 254, 784.
28. Shao, X.; Liu, W.; Xue, Q. *J Appl Polym Sci* 2004, 92, 906.
29. Shao, X.; Xue, Q.; Liu, W.; Teng, M.; Liu, H.; Tao, X. *J Appl Polym Sci* 2005, 95, 993.
30. Gonzalez, E. J.; White, G.; Wei, L. *J Mater Res* 2000, 15, 744.
31. Ji, Q. L.; Zhang, M. Q.; Rong, M. Z.; Wetzell, B.; Friedrich, K. *J Mater Sci* 2004, 39, 6497.